Analytical Sciences (2023) 39:537–546
https://doi.org/10.1007/s44211-022-00259-4

ORIGINAL PAPER

Observation of the phase-separation multiphase flow using a polyethylene glycol/phosphate mixed solutions and the aqueous two-phase distribution of red blood cells in the flow system

Kazushi Nishimura[1] · Chihiro Matsushita[1] · Kenichi Yamashita[2] · Masaharu Murata[3] · Kazuhiko Tsukagoshi[1]

Received: 23 September 2022 / Accepted: 23 December 2022 / Published online: 11 January 2023
© The Author(s), under exclusive licence to The Japan Society for Analytical Chemistry 2023

Abstract
Phase-separation multiphase flow at a liquid–liquid interface was successfully formed in an aqueous two-phase system of polyethylene glycol/phosphate mixed solutions when fed into a microchannel (100 μm wide and 40 μm deep) on a microchip and a fused-silica capillary tube (100 μm ID). As one example, tube radial distribution flow (annular flow) was observed when 10.0 wt% polyethylene glycol 6000 and 8.5 wt% dipotassium hydrogen phosphate aqueous solution containing 1.0 mM Rhodamine B was fed at 40 ℃, recorded by bright field microscopy. It exhibited a dipotassium hydrogen phosphate-rich inner phase and polyethylene glycol-rich outer phase. Effects of conditions including composition, flow rate, viscosity, and contact angle on tube radial distribution flow were analyzed. It was found out that although the viscosity of PEG-rich solution was much higher than that of phosphate-rich one, the phase configuration in tube radial distribution flow did not necessarily obey the viscous dissipation law in untreated microchannel and capillary tube, as well as for all the types of PEG/phosphate mixed solution the PEG-rich solution occupied the outer phase near the ODS-treated inner wall of both microchannel and capillary tube against the law. To assess the use of microfluidic flow in applications, we examined the distribution of red blood cells in the inner and outer phases fed into double capillary tubes with different inner diameters. Cell distribution was found to concentrate in the inner (dipotassium hydrogen phosphate-rich) phase compared to the outer (polyethylene glycol-rich) phase at a ratio of 1.8.

Keywords Phase-separation multiphase flow · Polyethylene glycol · Phosphate · Aqueous two-phase system · Tube radial distribution flow

Introduction

Aqueous two-phase systems (ATPS) have been useful in biotechnology as a non-denaturing and benign media for separation [1–6]. They result from the mixing of either two polymers, a polymer and kosmotropic salt, or a chaotropic and kosmotropic salt together under particular conditions. One of the studied aqueous biphasic systems since discovered is polyethylene glycol (PEG)/phosphate. This forms a two-phase system comprising an "upper phase" formed by the hydrophobic PEG and "lower phase" formed by the hydrophilic and denser phosphate solution. Successful extractions through liquid–liquid interfaces have been demonstrated using PEG/phosphate mixed solutions [7–9].

In our previous studies, a method of multiphase flow generation was presented using two-phase solutions, including water–hydrophilic–hydrophobic organic ternary [10], ionic liquid–water [11], and fluorocarbon–hydrocarbon organic solvent mixed solutions [12]. Using a batch vessel, it is possible to apply temperature and/or pressure changes to a homogeneous solution to induce upper and lower phases. We found that such phase transformations can be similarly induced when feeding into a microspace such as a microchannel on a microchip or a capillary tube, resulting in

✉ Kazuhiko Tsukagoshi
ktsukago@mail.doshisha.ac.jp

[1] Department of Chemical Engineering and Materials Science, Faculty of Science and Engineering, Doshisha University, Kyotanabe, Kyoto 610-0321, Japan

[2] Advanced Manufacturing Research Institute, National Institute of Advanced Industrial Science and Technology (AIST), 807-1 Shuku-Machi, Tosu, Saga 841-0052, Japan

[3] Innovation Center for Medical Redox Navigation, Kyushu University, 3-1-1 Maidashi, Higasi-ku, Fukuoka 812-8582, Japan

microfluidic flow with kinetic liquid–liquid interfaces [13, 14].

This novel type of multiphase flow was named as "phase-separation multiphase flow," contrasting with conventional immiscible multiphase flow. One specific microfluidic example is "tube radial distribution phenomenon" (TRDP) and the resulting "tube radial distribution flow" (TRDF) [15–18], which we have reviewed in previous studies [19–21]. In TRDF, a phase or kinetic liquid–liquid interface results within the microspace. Its unique properties with inner and outer phases have been applied to new types of chromatography, extraction, mixing, and microreactor systems [19–21].

These results are expected to form the first in a new field of TRDF and related research, as its novel microfluidic behavior is yet to be fully investigated. We believed it was vital to continue to examine fundamental properties of TRDF. Especially we needed more information concerning phase configuration of inner and outer phases in TRDF. In this study, despite recently publishing a technical report on PEG/citrate mixed solution where phase configuration was not examined in detail [22] and an extraction by using two polymers system of PEG/dextran mixed solution where viscous dissipation was strictly confirmed [23], a PEG/phosphate mixed solution ATPS formed from single polymer-dissolved aqueous solution [7–9] was used for examining TRDF (Fig. 1). The four types of PEG/phosphate mixed solutions, PEG6000/dipotassium hydrogenphosphate (K_2HPO_4) and PEG400/K_2HPO_4 as well as PEG6000/K_2HPO_4/dihydrogenphosphate (KH_2PO_4) and PEG400/K_2HPO_4/KH_2PO_4, were thoroughly explored by using untreated- and trichloro(octadecyl)silane (ODS)-treated microchannels and capillary tubes. Consequently, we found out a new phase configuration style in TRDF under certain experimental conditions.

The aqueous two-phase partitioning method developed by Albertsson does not use organic solvents or surfactants and has attracted attention as a separation and recovery method for biological components (proteins, cells, physiologically active substances, etc.) [7–9, 24–26]. Also, the distribution behavior of various cells in blood, including white blood cells, red blood cells, etc., has also been reported using an ATPS [27–29]. However, all of them are performed in a batch system, and there is little report on the method of separation and recovery in a flow. Therefore, we tried to separate and recover the biocomponents by phase separation in the flow using the aqueous two-phase partition method. Previously, we reported separation and recovery of proteins using the PEG/dextran system. However, dextran is difficult to handle due to its high viscosity and expensive. So, in this study, we tried to use the PEG/phosphate system in TRDF to investigate the separation and recovery of blood red cells as a model.

Experimental

Reagents and materials

Water was purified with an Elix 3 UV (Millipore Co., Billerica, MA). All reagents were commercially obtained and of

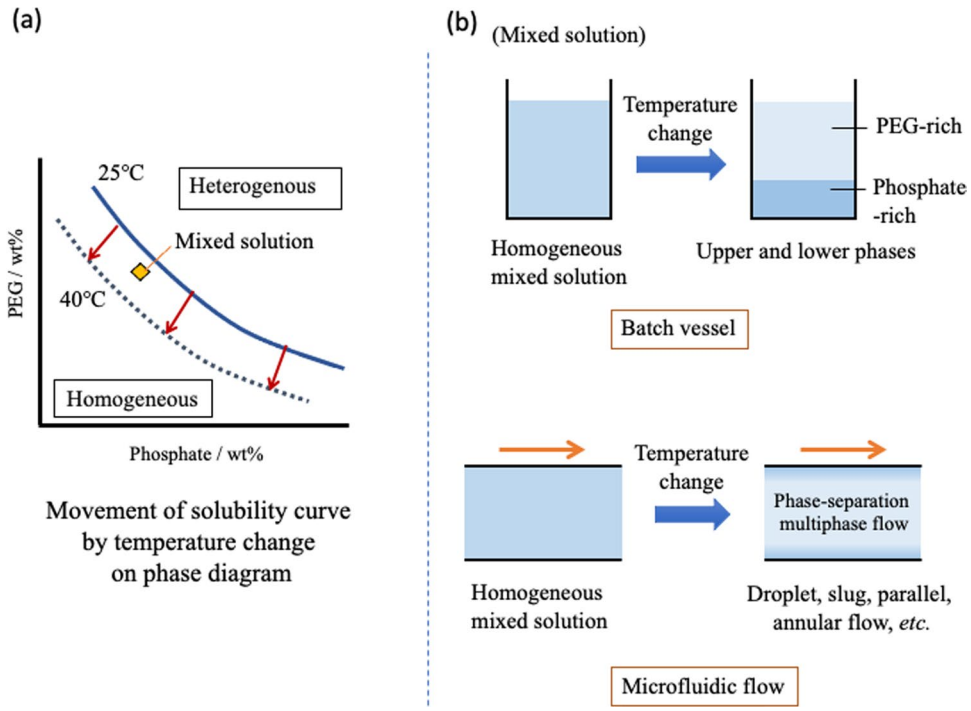

Fig. 1 **a** Phase diagram including solubility curve for PEG/phosphate mixed solution. **b** Process of phase-separation multiphase flow

analytical grade. PEG6000 or PEG400 (the number means molecular weight), Rhodamine B, K_2HPO_4, KH_2PO_4 were acquired from Wako Pure Chemical Industries, Ltd. (Osaka, Japan). ODS was purchased from Sigma Aldrich (Tokyo, Japan). A red blood cell solution was obtained from Nippon Bio-Test laboratories INC. (Saitama, Japan). A microchip made of glass incorporating a microchannel line (100 µm wide × 40 µm deep) was purchased from Microchemical Technology (Kanagawa, Japan). Fused-silica capillary tubes (75, 100, and 200 µm ID) were obtained from GL Sciences (Tokyo, Japan).

ODS-treated hydrophobic microchannel and capillary tube [30]

The hydrophobic-modified microchannel or capillary tube was prepared through the following procedure: 1 wt% ODS toluene solution was fed into a microchannel using a microsyringe pump at 1 µL min^{-1} flow rate for approx. 5 min. The channel was washed by feeding toluene from both ends at 50–100 µL min^{-1} followed by chloroform. The microchip was heated at 150 °C for 30 min to promote hydrophobicity in the microchannel. All other measurements in this study not referring to use of the ODS-treated microchannel or capillary tube were performed using untreated versions.

Viscosity measurement

Homogeneous solutions of all mixed solvent systems were converted to heterogeneous solution systems with two phases—upper and lower—by controlling the temperature in batch vessels. Viscosities of upper and lower phase solutions were measured with a viscometer (HAAKE RheoScope 1; Thermo Scientific, Sydney, Australia).

Bright-field microscope–charged-couple device (CCD) camera system

The ternary mixed solution with Rhodamine B was observed after delivery into the microchannel or capillary tube using a microscope (BX51; Olympus, Tokyo, Japan) and a CCD camera (JK-TU53H; Toshiba, Tokyo, Japan) for bright-field imaging (Fig. 2a). The addition of rhodamine B helped the

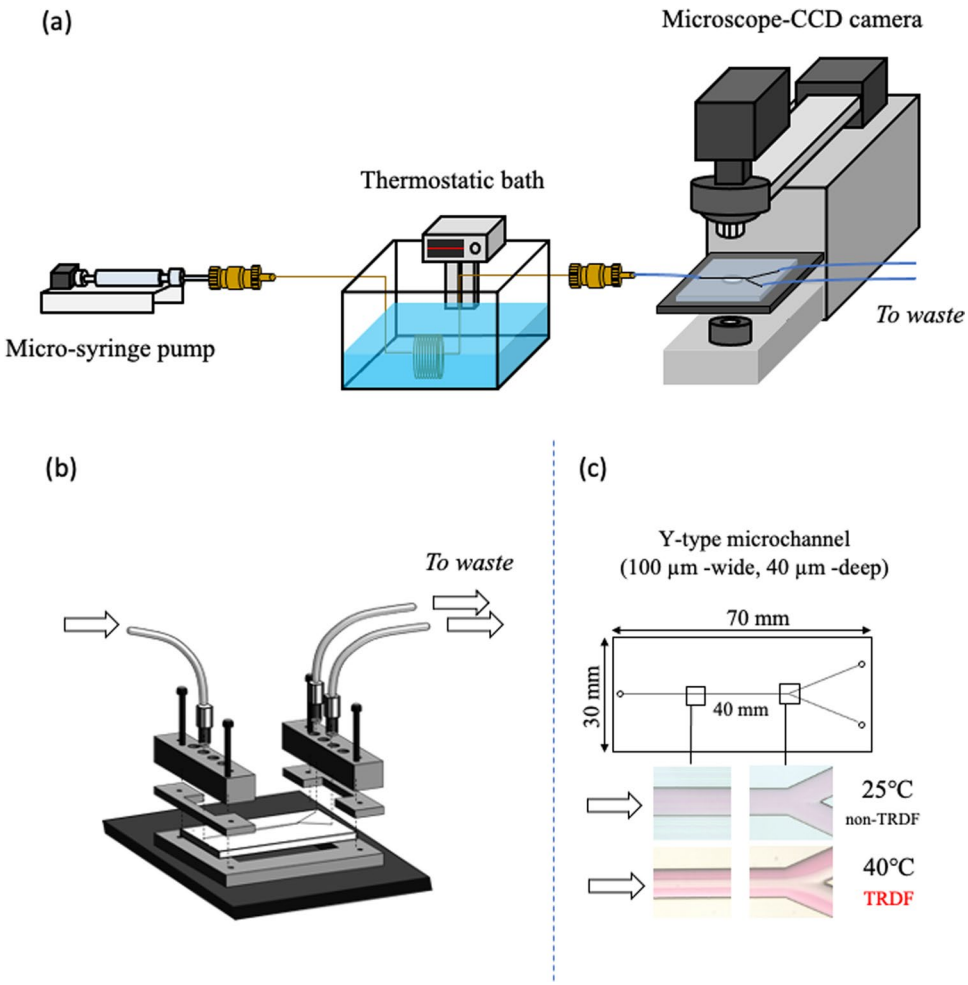

Fig. 2 Diagram of **a** bright-field microscope-CCD camera for observing microfluidic flow, **b** microchip and holder, and **c** Y-type microchannel on a microchip and images of non-TRDF and TRDF states. Mixed solution (PEG6000 10.0 wt% and K_2HPO_4/KHP_2O_4 8.5 wt%) containing 1.0 mM Rhodamine B was fed into the untreated channel at 10 µL min^{-1}

visualization of multiphase flow through microscope to recognize clearly, because rhodamine B (red color) distributed to PEG-rich phase than phosphate-rich one. The temperature of the capillary tube was controlled using a thermo-heater (Thermo Plate MATS-555RO; Tokai Hit Co., Shizuoka, Japan). Diagrams of (b) a microchip and holder and (c) Y-type microchannel on a microchip with non-TRDF and TRDF images are shown in Fig. 2.

Results and discussion

Phase diagram of PEG/phosphate mixed solution

We examined the phase diagram of PEG/phosphate mixed solution at 25 and 40 °C. Results for PEG6000/K_2HPO_4 and PEG400/K_2HPO_4 as well as PEG6000/K_2HPO_4/KH_2PO_4 and PEG400/K_2HPO_4/KH_2PO_4 are shown in Figs. 3 and 4, respectively. The pH values of PEG/K_2HPO_4/KH_2PO_4 and PEG/K_2HPO_4 were about 7 and 9, respectively. The wt% of the horizontal lines in Fig. 4 was calculated based on the total weight of K_2HPO_4 and KH_2PO_4 which were equimolar mixed. Solubility curves in the diagram indicate the boundary between the homogeneous solution and two-phase

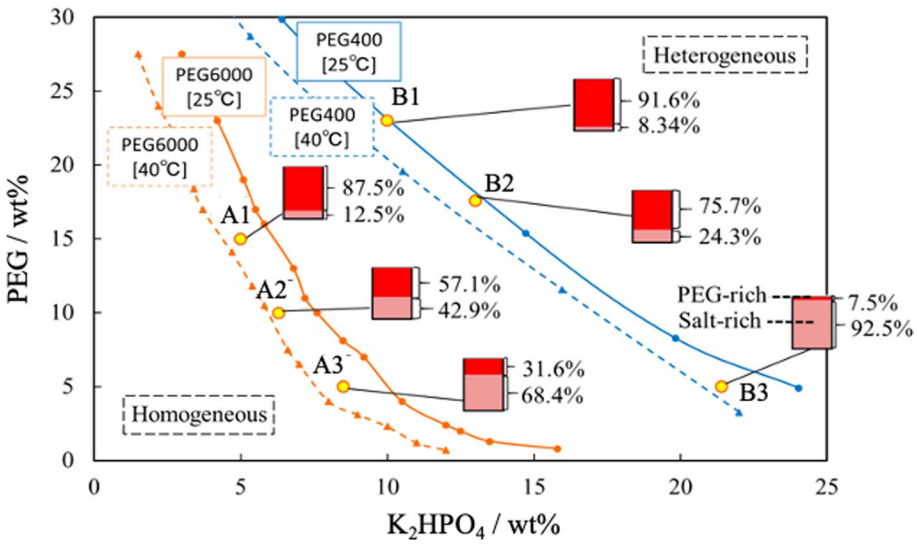

Fig. 3 Phase diagrams of PEG (PEG6000 or PEG400)/K_2HPO_4 mixed solution. Solubility curves shown by solid lines at 25 ℃ and dotted lines at 40 ℃. Mixed solutions A1, A2, A3, B1, B2, and B3 are homogeneous at 25 ℃, transforming to heterogeneous at 40 ℃. Volume ratios of upper and lower phases at 40 ℃ shown in percentages

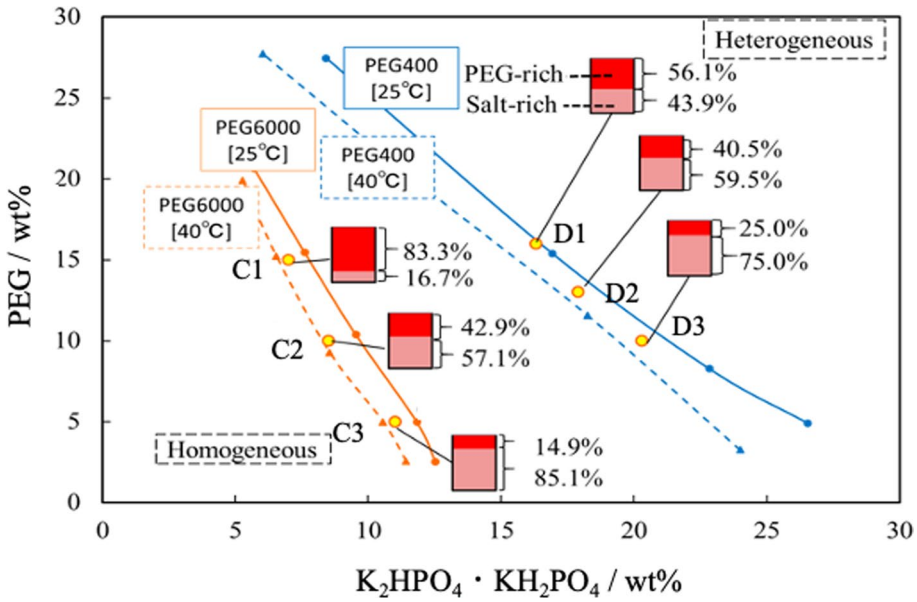

Fig. 4 Phase diagrams of PEG (PEG6000 or PEG400)/K_2HPO_4/KHP_2O_4 mixed solution. Solubility curves shown by solid lines at 25 ℃ and dotted lines at 40 ℃. Mixed solutions C1, C2, C-3, D1, D2, and D3 are homogeneous at 25 ℃, transforming to heterogeneous at 40 ℃. Volume ratios of upper and lower phases at 40 ℃ shown in percentages

heterogeneous solution. After heating from 25 to 40 °C, the A1–A3, B1–B3, C1–C3, and D1–D3 homogeneous mixed solutions become heterogeneous with an upper (PEG-rich solution) and lower (phosphate-rich solution) phase. The volume percentages of the heterogeneous solutions estimated through visual observation in a glass vessel are shown in the figures.

Phase configuration in TRDF

The relationship between shear rate and shear stress for upper and lower phase solutions in a batch vessel for the C2 mixed solution was examined (Fig. S1, Supporting Information). The well-defined linearity confirms its behavior as a Newtonian fluid. Viscosities of upper and lower phase solutions for mixed solutions A-D were measured and shown in Table 1. In all compositions the upper phase (PEG-rich) viscosities were much higher than lower phase (phosphate-rich).

We have previously discussed phase configuration in TRDF based on viscous dissipation and linear stability analysis [17, 31, 32]. When the difference in viscosity between the two phases is large, the higher viscosity phase forms the inner phase in TRDF regardless of volume ratio. The distribution pattern of solvents follows that expected by viscous dissipation law. In contrast, when the viscosity difference is small, the phase with larger volume forms the inner phase, matching estimations from linear stability analysis.

TRDF in microchannel

We first examined TRDF formation in untreated microchannel. The observed bright-field microscope photographs of PEG/phosphate mixed solution (C2 in Fig. 4) containing Rhodamine B in the microchannel at 25 and 40 °C are shown in Fig. 2c. Homogeneous flow was observed at 25 °C, while phase transformation into heterogeneous flow was seen at 40 °C with a liquid–liquid interface, indicated phase-separation multiphase flow or TRDF. The solutions A–D were fed at various flow rates (1–50 μL min^{-1}) to observe the change in flow type; TRDF, multiflow, slug flow, or unstable flow. (Fig. S2; Supporting Information). Figure 5a summarizes TRDF formation based on the basic data (Fig. S2) from the viewpoint of phase configuration of PEG-rich outer or PEG-rich inner. We observed two phase configurations in TRDF correlating to a PEG-rich inner with phosphate-rich outer phase and phosphate-rich inner with PEG-rich outer phase. That is, in spite of that PEG-rich phase was much high viscous, the phase configuration did not necessarily obey the viscous dissipation law.

We also examined the solutions using the ODS-treated microchannel for similar effects (Fig. S3; Supporting Information). We summarized TRDF formation based on the basic data (Fig. S3) in Fig. 5b, from the viewpoint of phase configuration of PEG-rich outer or PEG-rich inner. In contrast to the untreated microchannel, each configuration comprised a phosphate-rich inner phase and PEG-rich outer phase in the ODS-treated microchannel against the viscous dissipation law.

TRDF in fused-silica capillary tubes

We examined TRDF formation in untreated and ODS-treated fused-silica capillary tubes (100 μm ID, 360 cm length; observation point 100 cm from the capillary outlet) at 100 μL min^{-1}. In the untreated tube, TRDF was observed with a PEG-rich inner phase and phosphate-rich outer phase as well as phosphate-rich inner phase and PEG-rich outer phase configuration (Fig. 6a). In contrast, only a phosphate-rich inner phase and PEG-rich outer phase was seen in the ODS-treated tube (Fig. 6b). That is, the phase configuration in the untreated tube did not necessarily obey the viscous dissipation law, and the configuration in the ODS-treated tube showed only a phosphate-rich inner phase and PEG-rich outer phase against the law. It was confirmed that the similar configuration pattern in TRDC was observed for a microchannel and capillary tube mentioned above.

Phase configuration of PEG/phosphate mixed solution in TRDF using ODS-treated materials

Viscous dissipation and linear stability analysis cannot explain the TRDF phase configuration in PEG/phosphate mixed solution. We hence investigated the effect of inner wall characteristics of the microchannel and fused-silica capillary tube by comparing the contact angles of upper and lower phase solutions of A-D mixed solutions on untreated and ODS-treated glass plates. The obtained results that included the information of outer and inner phase configuration are summarized (Figs. S4 and S5; Supporting Information).

The contact angles of the upper and lower phases on ODS-treated glass were much higher than those on untreated. We hypothesized that a phase solution with a

Table 1 Viscosities of upper and lower phase for each solution composition

Solution composition	A1	A2	A3	B1	B2	B3	C1	C2	C3	D1	D2	D3
Upper phase /mPas	4.7	6.5	6.9	11.4	6.4	6.6	14.5	9.9	15.1	4.3	6.0	6.2
Lower phase /mPas	1.5	2.6	2.1	3.1	3.0	3.8	1.8	2.5	1.8	2.8	3.3	2.7

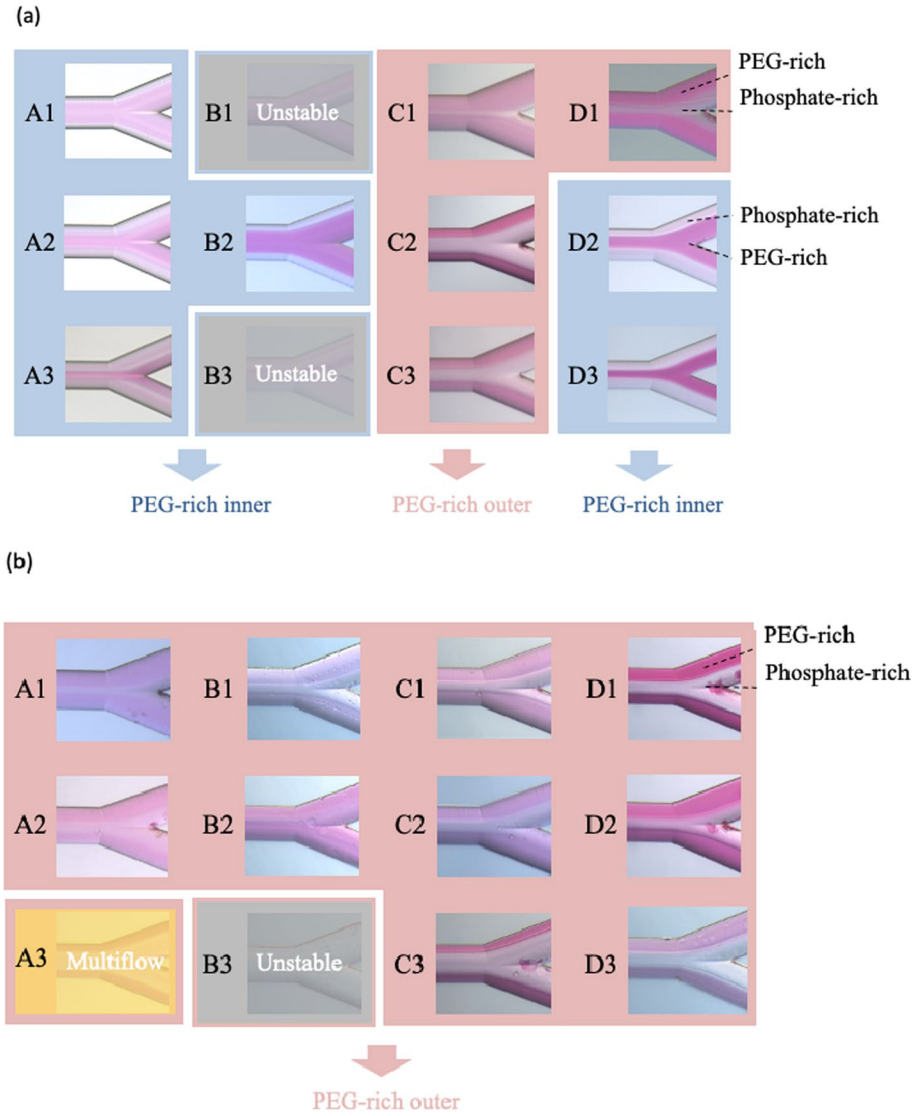

Fig. 5 Photographs of TRDF configuration of PEG-rich inner or PEG-rich outer phase **a** in untreated Y-type microchannel at a flow rate of 5 μL min^{-1} and **b** in ODS-treated Y-type microchannel at a flow rate of 20 μL min^{-1} for D3, 1 μL min^{-1} for A1, A2, A3, and C1, and 5 μL min^{-1} for others

smaller contact angle may be placed as an outer phase near the inner wall. However, a clear relationship between TRDF phase configuration and contact angle was not seen, implying the contact angle effect for a plate in air deviates from that for microchannel and capillary tube inner walls.

Nonetheless, overall we can consider the ODS-treated inner wall to be more hydrophobic than the untreated one, so that the PEG-rich phase comprising more polymers has more affinity to the treated wall than the phosphate-rich phase comprising ions has. Therefore, it may be concluded for the moment, that although the viscosity of PEG-rich solution was much higher than that of phosphate-rich one, the phase configuration in TRDC did not necessarily obey the viscous dissipation law in untreated microchannel and capillary tube, as well as for all the types of PEG/phosphate mixed solution the PEG-rich solution occupied the outer phase near the ODS-treated inner wall of both microchannel and capillary tube against the law at least under certain experimental conditions. In the future, we will investigate the phase configuration of PEG/phosphate mixed solution in TRDF from the viewpoints of dynamic friction, polymer rheology, and hydrogen bonding properties of PEG with the inner wall surface.

Distribution of red blood cells in upper and lower phases

One application of ATPS including PEG/phosphate mixed solution is separation of biomolecules and biocells [7–9, 24–26]. In this study we modeled the separation of red blood cells in inner and outer phases in TRDF using a Y-type microchannel on a microchip and microflow system for different diameter double tubes. First, we examined the absorption spectra and calibration curve for red blood cells at 406 nm (Fig. S6, Supporting information). We then examined the distribution ratio of red blood cells in upper/lower

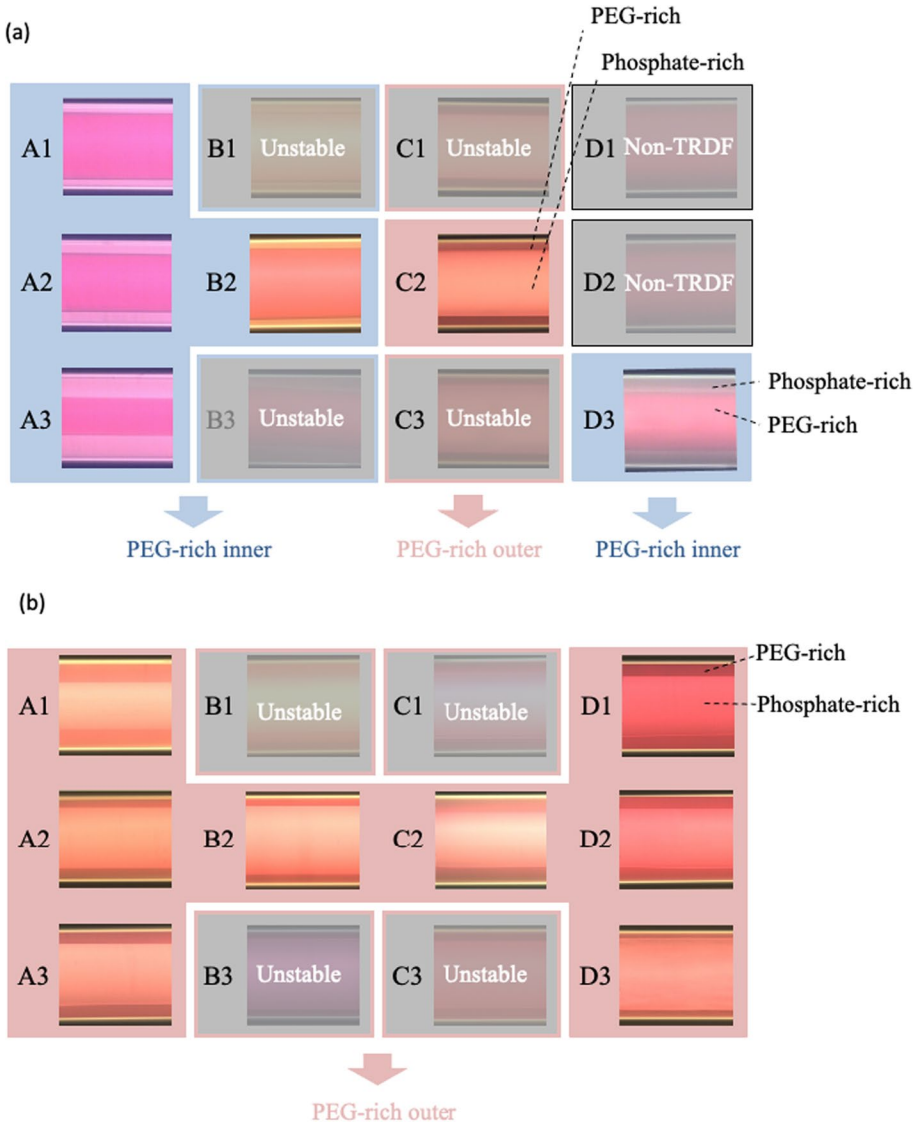

Fig. 6 Photographs of TRDF configuration of PEG-rich inner or PEG-rich outer phase **a** in untreated fused-silica capillary tube (100 µm ID, length 360 cm; observation point 100 cm from the capillary outlet) at a flow rate of 100 µL min^{-1} and **b** in ODS-treated fused-silica capillary tube (100 µm ID, length 360 cm; observation point 100 cm from the capillary outlet) at a flow rate of 100 µL min^{-1}

phases in a batch vessel using the calibration curve for C2 mixed solution. In the results, red blood cells were concentrated in the phosphate phase at a distribution ratio of 1.9 compared to the PEG phase. The number of 1.9 corresponds to distribution coefficient.

Effect of TRDF on red blood cell concentration

Different pressure losses were generated in the Y-type channels through the following set-up [22]. Two PTFE tube types, one with 500 µm ID (25.4 cm length) and another with 250 µm ID (50 cm length), were connected to two separate microchannels on a Y-type microchip to control the pressure loss difference ΔP (ca. 3.4 kPa). The results indicate that the homogeneous mixed solution C2 transformed into two phases in the microchannel at 40 °C, allowing for separation in the Y-type channels as shown in Fig. 7. Figure 8 shows the successful collection of red blood cells in the phosphate-rich phase using TRDF and pressure loss difference.

Figure 9a shows a diagram of the microflow separation system comprising double capillary tubes [23, 33] with 75, 100, and 200 µm ID and the experimental conditions. The observed TRDF after feeding the PEG/phosphate mixed solution C2 into the large capillary is shown in Fig. 9b. The system allowed the inner phosphate-rich and outer PEG-rich phases to separate by following the inner and outer capillaries, respectively. Conditions determining the flow from capillary A to B were found experimentally after varying the length of capillary C.

Red blood cell distribution between the inner and the outer TRDF phases was similarly examined through the microflow separation system, recovered continuously in capillaries B and C, respectively. Blood cells were seen to concentrate in the inner phosphate-rich phase at a distribution ratio of 1.8

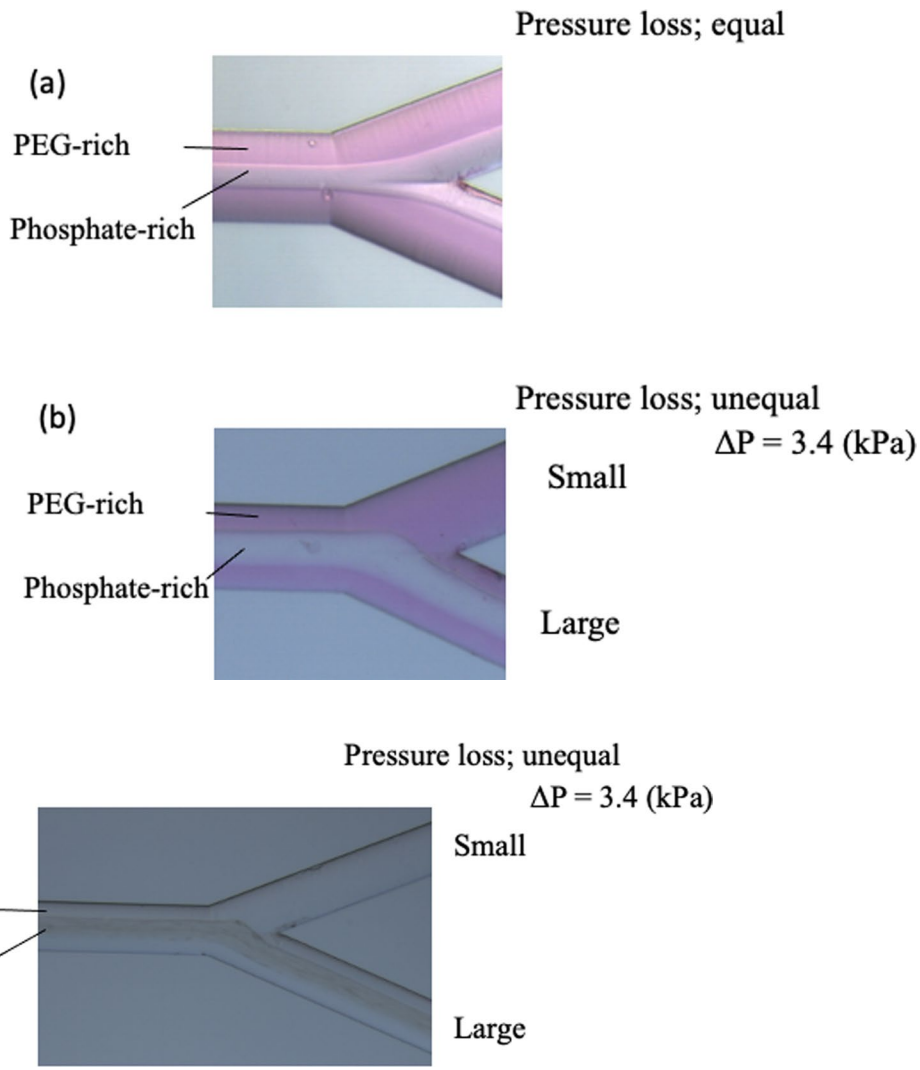

Fig. 7 Bright-field images of microfluidic flow in Y-type microchannel for solution C2 (PEG6000 10.0 wt% and K_2HPO_4/KHP_2O_4 8.5 wt%) containing 1.0 mM Rhodamine B at 40 °C and flow rate of 10 μL min^{-1} for **a** equal and **b** unequal (ΔP; 3.4 kPa) pressure loss

Fig. 8 Concentration of red blood cells in Y-type microchannel through TRDF formation and pressure loss difference (ΔP; 3.4 kPa). Mixed solution C2 (PEG6000 10.0 wt% and K_2HPO_4/KHP_2O_4 8.5 wt%) containing 1.2 μL mL^{-1} of red blood cells was fed at a flow rate of 10 μL min^{-1}, heated from 25 to 40 ℃ to produce TRDF. Rhodamine B was not used in the system

compared to the outer phase, measured by absorption spectrophotometry calibration. The number of 1.8 corresponds to distribution coefficient. This closely matched the ratio obtained using the batch vessel. The aqueous two-phase partitioning method has attracted attention as a separation and recovery method. However, all of them are performed in a batch system, and there is little report on the method of separation and recovery in a flow. The results obtained here must give a clue to provide a new flow separation system for biological components.

Conclusions

We reported the first results of phase-separation multiphase flow including TRDF achieved through ATPS comprising PEG/phosphate mixed solutions fed through a microchannel and a capillary tube. The effect of composition, flow rate, viscosity, contact angle and other conditions were analyzed. It was found out that for all the types of PEG/phosphate mixed solution the PEG-rich solution occupied the outer phase near the ODS-treated inner wall of both a microchannel and a capillary tube. In addition, blood red cells fed into a microflow separation system incorporating double capillary tubes were seen to concentrate in the phosphate-rich solution during TRDF. The developed microflow system will be useful for the separation and extraction of similar cells and biomolecules.

Supplementary Information The online version contains supplementary material available at https://doi.org/10.1007/s44211-022-00259-4.

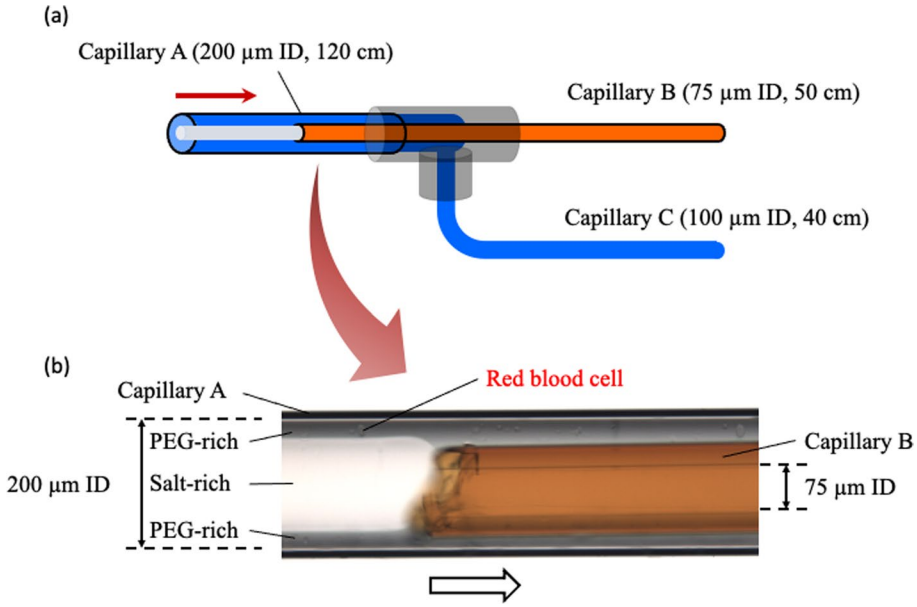

Fig. 9 Collection of red blood cells in different diameter double capillary tubes through TRDF formation. Mixed solution C2 (PEG6000 10.0 wt% and K_2HPO_4/KHP_2O_4 8.5 wt%) containing 1.2 µL mL^{-1} of red blood cells was fed at a flow rate of 100 µL min^{-1}, heated from 25 to 40 ℃ to produce TRDF. Rhodamine B was not used in the system

Acknowledgements This work was supported by a Grant-in-Aid for Scientific Research (C) from the Ministry of Education, Culture, Sports, Science, and Technology, Japan (MEXT) (No. 17H03083).

Data Availability Statement The microflow system gave a useful clue to develop the separation and extraction of cells and biomolecules in a microspace.

Declarations

Conflict of interest The authors declare no competing financial interest.

References

1. H. Tani, T. Kamidate, H. Watanabe, Hiroto, Anal. Sci. **14**, 857 (1998). https://doi.org/10.2116/analsci.14.875
2. M. Van Berlo, M. Ottens, K.C.A.M. Luyben, L.A.M. van der Wielen, J. Chromatogr. B **743**, 317 (2000). https://doi.org/10.1016/S0378-4347(00)00173-0
3. G.D. Rodrigues, L. Rodrigues de Lemos, L.H. Mendes da Silva, M.C. Hespanhol da Silva, Anal. Sci. **28**, 1213 (2012). https://doi.org/10.2116/analsci.28.1213
4. F. Ruiz-Ruiz, J. Benavides, O. Aguilar, M. Rito-Palomares, J. Chromatogr. A **1244**, 1 (2012). https://doi.org/10.1016/j.chroma.2012.04.077
5. A. Hamta, M.R. Dehghani, J. Mol. Liq. **231**, 20 (2017). https://doi.org/10.1016/j.molliq.2017.01.084
6. J.A. Asenjo, B.A. Andrews, J. Chromatogr. A **1218**, 8826 (2011). https://doi.org/10.1016/j.chroma.2011.06.051
7. S.O. Enfors, K. Koehler, A. Veide, Andres, Bioseparation **1**, 305 (1990)
8. D.F. Colosimo, V.-P.-R. Minim, M.C.T.R. Vidigal, L.A. Minim, L. Antonio, Chem. Eng. Res. Des. **182**, 478 (2022). https://doi.org/10.1016/j.cherd.2022.04.012
9. R.J. Anderson, C. Delgado, D. Fisher, J.M. Cunningham, G.E. Francis, Anal. Biochem. **193**, 101 (1991). https://doi.org/10.1016/0003-2697(91)90048-X
10. H. Kan, K. Yamada, N. Sanada, K. Nakata, K. Tsukagoshi, Anal. Sci. **34**, 239 (2018). https://doi.org/10.2116/analsci.34.239
11. K. Nagatani, Y. Shihata, T. Matsushita, K. Tsukagoshi, Anal. Sci. **32**, 1371 (2016). https://doi.org/10.2116/analsci.32.1371
12. K. Kitaguchi, N. Hanamura, M. Murata, M. Hashimoto, K. Tsukagoshi, Anal. Sci. **30**, 687 (2014). https://doi.org/10.2116/analsci.30.687
13. M. Murakami, N. Jinno, M. Hashimoto, K. Tsukagoshi, Anal. Sci. **27**, 793 (2011). https://doi.org/10.2116/analsci.27.793
14. N. Jinno, M. Murakami, K. Mizohata, M. Hashimoto, K. Tsukagoshi, Analyst **136**, 927 (2011). https://doi.org/10.1039/C0AN00820F
15. N. Jinno, M. Murakami, K. Mizohata, M. Hashimoto, K. Tsukagoshi, Analyst **135**, 927 (2011). https://doi.org/10.1039/C0AN00820F
16. S. Fujinaga, M. Hashimoto, K. Tsukagoshi, J. Mizushima, J. Chem. Eng. Jpn. **48**, 947 (2015). https://doi.org/10.1252/jcej.15we039
17. S. Fujinaga, M. Hashimoto, K. Tsukagoshi, J. Mizushima, Anal. Sci. **32**, 455 (2016). https://doi.org/10.2116/analsci.32.455
18. K. Yamada, H. Kan, K. Tsukagoshi, Talanta **189**, 89 (2018). https://doi.org/10.1016/j.talanta.2018.02.046
19. K. Tsukagoshi, Anal. Sci. **30**, 65 (2014). https://doi.org/10.2116/analsci.30.65
20. K. Tsukagoshi, J. Flow Inject. Anal. **32**, 89 (2015)
21. K. Tsukagoshi, Bunseki-Kagaku (Review) **71**, 25 (2022)
22. A. Yoshioka, K. Tsukagoshi, K. Tsuchiya, K. Hirota, K. Yamashita, M. Murata, Anal. Sci. **35**, 1279 (2019). https://doi.org/10.2116/analsci.19A001
23. N. Imanishi, T. Yamasaki, K. Tsukagoshi, M. Murata, Anal. Sci. **34**, 953 (2018). https://doi.org/10.2116/analsci.18P105
24. P.A. Albertsson, *Partition of Cell Particles and Macromolecules* (Wiley, New York, 1986)
25. R. Kuboi, H. Tanaka, I. Komasawa, Kogaku Kogaku Ronbunshu **16**, 755 (1989). https://doi.org/10.1252/kakoronbunshu.16.755
26. E. Sumida, Y. Iwasaki, K. Akiyoshi, S. Kasugai, J. Pharmacol. Sci. **101**, 91 (2006). https://doi.org/10.1254/jphs.FP0060062
27. H. Walter, F.W. Selby, J.M. Brake, Biochem. Biophys. Res. Commun. **15**, 497 (1964)
28. H. Walter, R. Winge, F.W. Selby, Biochim. Biophys. Acta **109**, 293 (1965)

29. H. Walter, F.W. Selby, R. Garza, Biochim. Biophys. Acta **136**, 148 (1967)
30. B. Yamawaki, R. Mori, K. Tsukagoshi, K. Tsuchiya, K. Yamashita, M. Murata, Anal. Sci. **35**, 249 (2019). https://doi.org/10.2116/analsci.18P393
31. M.C. Williams, AlChE J. **21**, 1204 (1975)
32. D.D. Joseph, Y. Renardy, M. Renardy, J. Fluid Mech. **141**, 309 (1984)
33. K. Yamada, N. Jinno, M. Hashimoto, K. Tsukagoshi, Anal. Sci. **26**, 507 (2010). https://doi.org/10.2116/analsci.26.507

Springer Nature or its licensor (e.g. a society or other partner) holds exclusive rights to this article under a publishing agreement with the author(s) or other rightsholder(s); author self-archiving of the accepted manuscript version of this article is solely governed by the terms of such publishing agreement and applicable law.